

## Effects of butyl acrylate modified polypropylene on structural and thermal properties of foamed polypropylene

Lifen Su,<sup>1,2</sup> Wei Zhang,<sup>1</sup> Ru Xia,<sup>1</sup> Jibin Miao,<sup>1</sup> Bin Yang,<sup>1</sup> Jiasheng Qian,<sup>1</sup>  
Fang Ruan,<sup>1</sup> Zhengzhi Zheng<sup>1</sup>

<sup>1</sup>Anhui Province Key Laboratory of Environment-Friendly Polymer Materials, School of Chemistry and Chemical Engineering, Anhui University, Hefei 230601, China

<sup>2</sup>Key Laboratory of Renewable Energy, Chinese Academy of Sciences, Guangzhou 510640, China

Correspondence to: L. Su (E-mail: ausulf@gmail.com) and R. Xia (E-mail: xiarucn@sina.com)

**ABSTRACT:** In this work, the melt strength of PP matrix was reinforced by crosslinking-modified PP (CM-PP) which was yielded by peroxide-initiated crosslinking of linear PP with butyl acrylate (BA). The nano-silica aerogel (nano-SiO<sub>2</sub>) worked as a nucleating agent for foaming. The effects of CM-PP with the various contents of BA on the foaming behavior and thermal property of PP were studied by measurements of density, thermal conductivity, Vicat softening temperature and SEM. The results showed that the foamed PP got the best properties when the crosslinking PP modified with the weight ratio of butyl acrylate was 10 wt %. The density of the obtained foamed PP with uniform closed cells was as low as 0.23 g/cm<sup>3</sup>, the thermal conductivity was 0.044 W/(m K), and the Vicat softening temperature was 120 °C. © 2016 Wiley Periodicals, Inc. *J. Appl. Polym. Sci.* **2016**, *133*, 44340.

**KEYWORDS:** crosslinking; foams; properties and characterization; thermal properties

Received 25 March 2016; accepted 4 August 2016

DOI: 10.1002/app.44340

### INTRODUCTION

As an environment-friendly material, foamed polypropylene (PP) is a kind of solid/gas composites with a large number of cells filled internal resin.<sup>1,2</sup> The composites provides a new platform for applications such as thermal insulators, package, and energy absorption because of the lower density, larger energy absorption capacity, and excellent thermal stability of foamed PP.<sup>3,4</sup> The further application of PP foams is restricted by the difficult preparing technology due to the high crystallization temperature of PP as 165 °C, and the weak melt strength leads to a narrow processing temperature range as about 4 °C.<sup>5–8</sup> Therefore, the reinforce of the melt strength is an effective approach to improve the foaming behavior of PP.

The chemical modification of linear PP (L-PP) by peroxide-initiated crosslinking can improve the melt viscoelasticity and extensional viscosity effectively.<sup>9</sup> The product's molecular weight and branching distribution of PP were controlled by the balance of chain scission and crosslinking which were involved in these solvent-free processes simultaneously.<sup>10,11</sup> Liu and Chuai<sup>12</sup> prepared silane crosslinked PP by grafting of silane onto the backbone of PP in a melt process using a twin-screw extruder and then crosslinking in hot water. The results showed that the strength was enhanced from 0.06 MPa to 0.32 MPa, which can effectively promote the formation of foam with an optimum

melt flow rate, sag resistance, and tension strength at a high temperature. Feng and Wang<sup>13</sup> prepared the crosslinking PP through a two-step process by electron beam irradiation, and then prepared PP foams by blending the crosslinking PP. The results showed that the melt strength of PP matrix was enhanced from 0.05 MPa to 0.30 MPa, and the obtained PP foams with a maximum expansion ratio (12.1%) and minimum density (0.09 g/cm<sup>3</sup>) were produced under the optimum condition of 240 °C for 300 s. As the foaming temperature or time increased, the cell size increased, and the cell density decreased regularly. However, the coalescence and even the collapse of the cells will be caused by the excessive high foaming temperature (>250 °C) and long foaming time (>300 s). Besides, many studies about high melt viscosity branching have been reported to improve the cellular structure of the foamed PP.<sup>14–18</sup> However, the researches on the relationship between structure and thermal conductivity of foamed PP were very limited.<sup>19</sup>

In this report, we developed a new strategy to improve the melt strength of PP by blending CM-PP modified with butyl acrylate (BA). In general, the products derived from crosslinking modification with the butyl acrylate groups are comprised of a linear chain of a relatively low molecular weight chain and a high molecular weight chain population that contains a disproportionate amount of long chain branching. The effects of CM-PP

modified with different butyl acrylate contents on the relationship of the structure and thermal conductivity of PP matrix were studied.

## EXPERIMENTAL

### Materials

Linear PP (L-PP, SP179) and PP (SEP-540) with little branch were obtained by Qilu Branch of Sinopec Corp. and Honam Petrochemical Corp., respectively. The nano-SiO<sub>2</sub> aerogel powders were synthesized in the authors' laboratory.<sup>20</sup> The azodicarbonamide (AC, AZ-H-25, AR) was used as foaming agents, which was purchased from Shanghai Jieyu Industry and Trade Corp. Besides, the crosslinking agents including dicumyl peroxide (DCP, AR) and butyl acrylate (BA, AR) were provided by Shanghai Shanpu Chemical Corp. and Tianjin Guangfu Chemical Industry Research Institute, respectively. The thermal stabilizers including zinc oxide (ZnO, AR) and zinc stearate (ZnSt, CP) were purchased from Tianjin Baishi Chemical Corp. and Tianjin Guangfu Chemical Industry Research Institute, respectively. The ZnO and ZnSt were used as promoters which can promote the decomposition of foaming agent. The active free radicals generated by the dissociation of DCP were used as an initiator of crosslinking reactions.

### Materials Preparation and Foaming

Crosslinking-modified PP (CM-PP) was fabricated by immersing the L-PP powder (100 g) into the acetone solution dispersed with DCP (0.2 g) and different contents of BA for 2 h. The weight ratio of BA/CM-PP was varied from 0, 5, 10, 15, 20, 25, and 30. After the evaporation of the solvent, the obtained mixture was put into the Haake torque rheometer for 10 min when the temperature was 180 °C and the screw speed was 60 rpm.

The PP (SEP-540) matrix, CM-PP, nano-SiO<sub>2</sub> (4 wt %)<sup>21</sup> were put into the Haake torque rheometer when the temperature was 170 °C with 60 rpm. After the mixture had melted into a homogeneous phase, the AC (6 wt %), ZnO (2 wt %), and ZnSt (3 wt %) was added in turn with an interval of 3 min. The weight ratio of CM-PP/(PP + CM-PP) was 20%. The obtained mixture was transmitted into the preheated mold cavity with the size as 150 × 150 × 1.5 mm and foamed at 190 °C with 10 MPa for 100 s in the plate vulcanizing machine (QLB-25D/Q, Shanghai Wings Rubber and Plastic Machinery Corp. LTD). The foamed PP with excellent properties was obtained after the complete decomposition of foaming agents.

### Characterization Methods

The melt flow rate (MFR) of PP matrix was tested by the melt flow rate detector (ZRZ1452, Shenzhen SANS Testing Machine Corp.) under the condition of 2.16 kg and 230 °C. The melt strength (MS) was calculated by the eq. (1)<sup>22</sup> as following.

$$MS = \frac{8.5 \times 10^{-2} \Delta l^2 r_0^2}{MFR} \quad (1)$$

MS is the melt strength of PP matrix;  $\Delta l$  is the length of extrudate when the diameter of the extrudate reduced to 50%;  $r_0$  is the radius of the extrudate when the sample just leaves the extruding die.

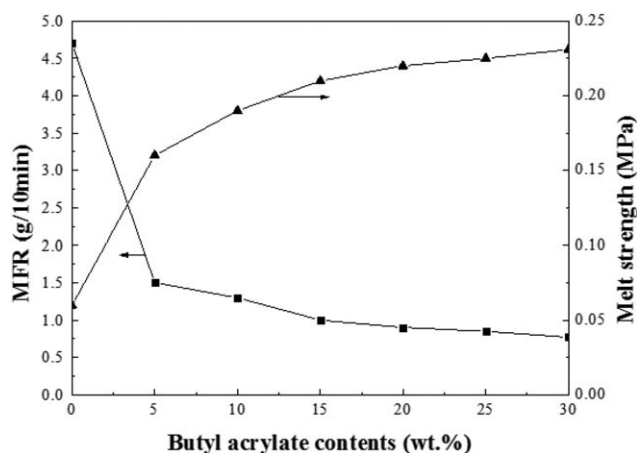


Figure 1. Effect of BA contents on the rheological behavior of PP matrix.

The crystal melting temperature of the CM-PP was estimated from thermogravimetric and differential analyses (TG-DTA, SETARAM Labsys, France), in nitrogen during heating to 200 °C at 10 °C/min. The PP samples were analyzed using the ATR-FTIR (Nicolet iS10, ThermoFisher, America) by shaping the sample into a flake (20 × 20 × 1 mm) in the plate vulcanizing machine.

The density ( $\rho$ ) of the PP foams was calculated by the equation  $\rho = m/v$ , the weight ( $m$ ) was measured by the electronic balance (AUY220) and the volume ( $v$ ) was calculated by measuring the length, width and height of foamed PP. The Vicat softening temperature was carried out by the thermal deformation testing machine (XIOU, China) with a GB/T1633-2000. The thermal conductivity was tested by the TCi thermal analyzer (C-Therm Technologies Ltd., Canada) with the ambient temperature as 17.8 °C.

The cross-section morphology of the foamed PP was investigated by field emission scanning electron microscopy (FE-SEM, Hitachi S-4800, Japan) after the samples soaking in the liquid nitrogen for 10 min and broken. The cell density of foamed PP was calculated by the eq. (2)<sup>22,23,24</sup> as following.

$$N_0 = \left( \frac{nM^2}{A} \right)^{\frac{2}{3}} \cdot \varphi \quad (2)$$

$N_0$ , cell density, which is defined as the number of cells per unit volume of original (unfoamed) sample;  $n$ , the number of cell in the SEM images of foam;  $A$ , the area of the SEM images; expansion ratio  $M$ , the magnification factor;  $\varphi$  is the volume expansion ratio, which was calculated by the formula:  $\varphi = \frac{\rho_0}{\rho_1}$ , and the  $\rho_0$  was the density of the unfoamed PP, the  $\rho_1$  was the density of the foamed PP.

## RESULTS AND DISCUSSION

### Rheological and Structural Properties

The influences of BA contents on the MFR and the melt strength of the PP matrix are shown in Figure 1. It can be observed that the MFR of PP matrix decreases sharply with 5 wt % BA, and then slows down as an increase of BA content up to 30 wt %, which indicates that the BA modified CM-PP is contributed to the processability of foamed PP. The melt

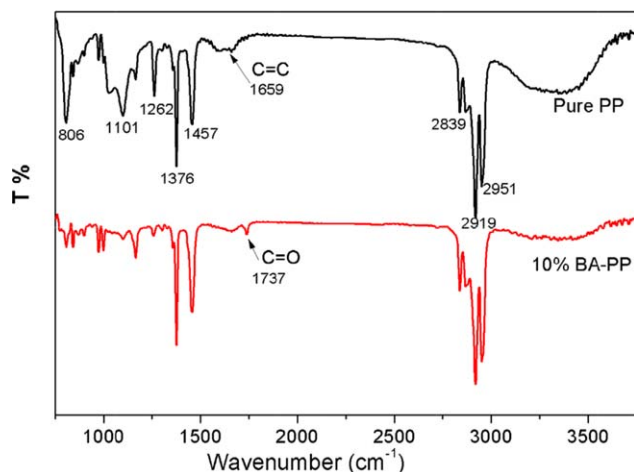
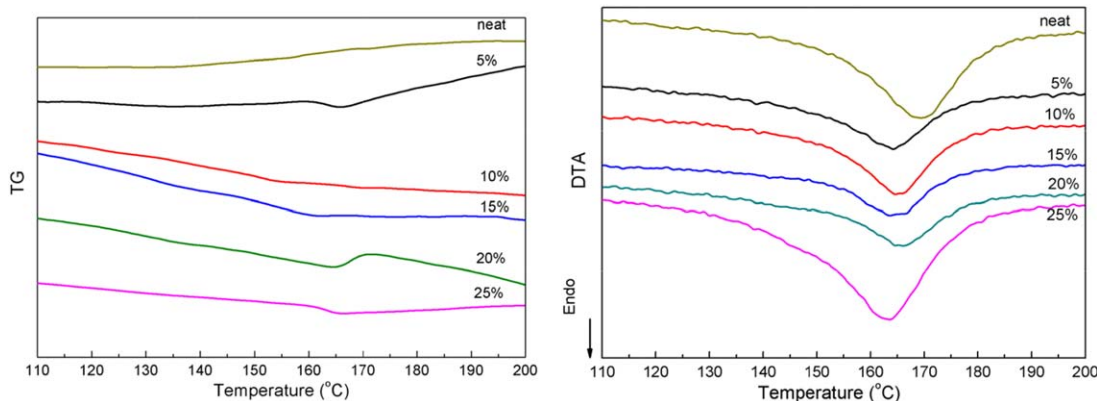


**Figure 2.** Comparative IR spectra of pure PP and CM-PP with 10% BA. [Color figure can be viewed at [wileyonlinelibrary.com](http://wileyonlinelibrary.com).]

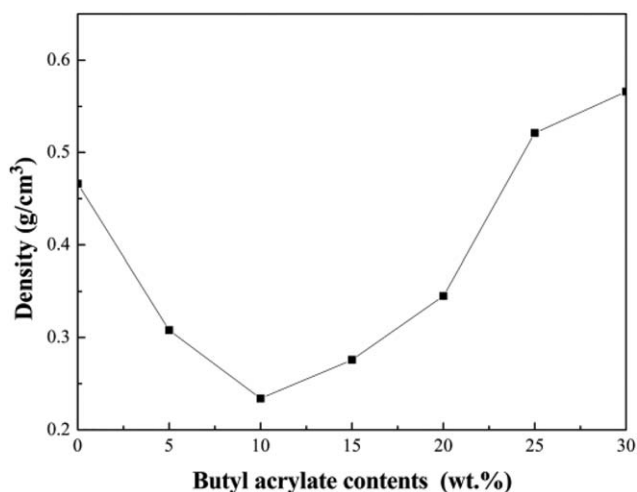
strength of PP matrix increases quickly with the addition of 10 wt % BA and then becomes slowly with more BA contents. It is mainly due to that the number of free radicals produced by the decomposition of DCP limits the number of the reactive sites on the PP molecular chain, which impacts on the crosslinking reaction during the CM-PP yielding process. Therefore, the results of MFR and melt strength of PP matrix are both indicating that the BA modified CM-PP plays an important role in the foaming process.

Figure 2 compares the IR spectra of the pure PP and 10% BA modified PP. The peaks of pure PP have a good agreement with those of reference spectra of PP. However, the C=O stretch at  $1737\text{ cm}^{-1}$  was presented and the C=C peak at  $1659\text{ cm}^{-1}$  disappeared in the CM-PP with 10% BA, which indicate that the C=O group was grafted onto the molecular chain of PP successfully by opening the C=C group of both BA and PP to form the crosslinking structure without any residual BA in the CM-PP resin.

The TG-DTA thermograms of CM-PP with different BA content are shown in Figure 3. The TG curves show that the weight loss



**Figure 3.** TG-DTA thermograms of PP modified with different BA content. [Color figure can be viewed at [wileyonlinelibrary.com](http://wileyonlinelibrary.com).]



**Figure 4.** Density of foamed PP modified with different BA contents.

is little during the heating process for all samples. It can be observed that the crystal melting peak of the PP matrix shifted to lower temperatures with an increasing BA contents up to 25 wt % from the DTA thermograms. It might be that the crosslinking structures of the CM-PP were formed by opening the C=C groups of BA and linear PP to initiate crosslinking reaction, which leads to increasing the flexibility of PP matrix and lowering the crystal melting temperature.

#### Density

The effects of CM-PP modified with different BA contents on the density of foamed PP are shown in Figure 4. The density of foamed PP decreases firstly with an increase of BA contents from 0 to 10 wt %, and the lowest density as  $0.23\text{ g/cm}^3$  is obtained when the PP matrix modified by blending CM-PP with 10 wt % BA content. It can be attributed to that the CM-PP improved the melt strength of PP matrix effectively. The BA worked as a double bond function monomer can promote the formation of interpenetrating network and cut off the degradation of PP.<sup>25</sup> The CM-PP will form a crosslinking grid structure in the PP matrix, which can improve the melt strength of PP.<sup>26</sup> It has good agreement with the above results of the rheology.

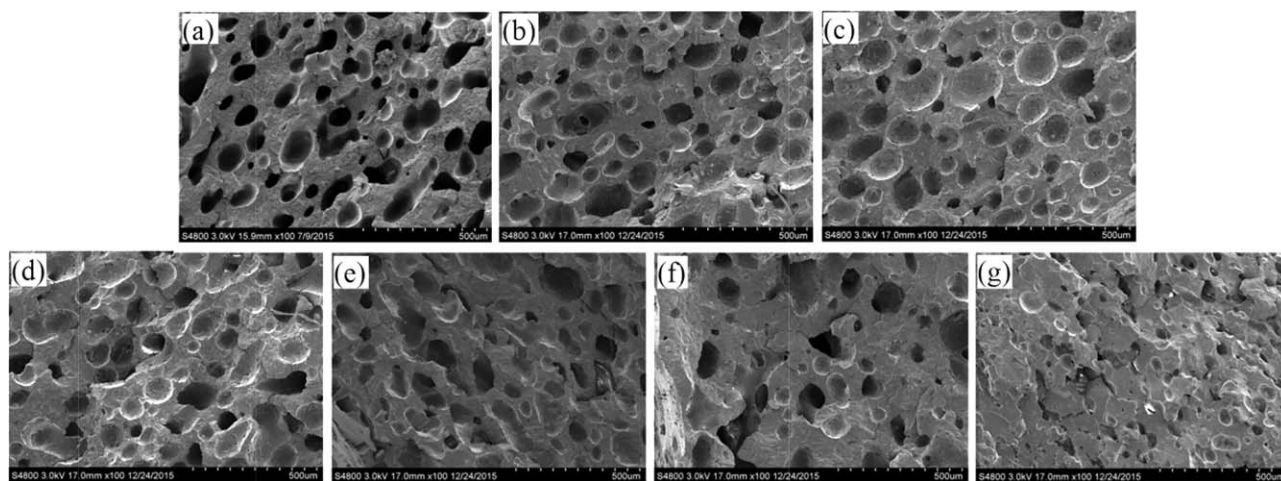


**Figure 5.** The cell morphology of foamed PP with CM-PP modified with different BA contents: (a) 0, (b) 5 wt %, (c) 10 wt %, (d) 15 wt %, (e) 20 wt %, (f) 25 wt %, (g) 30 wt %.

However, when the BA content is more than 10 wt %, the density increases due to that the excessive crosslinking density of CM-PP leads to the excessive melt strength of PP matrix,<sup>19</sup> which results in restricting the formation and expanding of bubbles, and reducing the cell density of foamed PP during the expansion process.<sup>6</sup> It is owing to that the increase of crosslinking structure will prevent the movement of the PP molecular chain and increase the intermolecular forces. The formation and expansion of the cellular structure will be limited by excessive melt strength of PP matrix, which leads to decreasing the number and sizes of the cells. Therefore, the lightweight PP foams with excellent foaming property are obtained under moderate melt strength of PP matrix.

### Morphology Analysis

The SEM micrographs of the foamed PP modified by CM-PP with different BA contents are shown in Figure 5. It can be observed that the foamed PP has large numbers of uniform insular cells with the diameters of cells at the range of 50 to 200  $\mu\text{m}$ . The morphology of the foamed PP shows that the structure of foamed PP without BA contents is mainly comprised of an open cell. When the CM-PP modified with 10 wt % BA, the numerous uniform closed cells with a thin solid cell walls are obtained. The foamability of PP with more uniform cellular structure was improved with an increase of BA up to 10 wt %, and then weakened with an excess of BA contents. It can be attributed to that the melt strength of PP matrix improved by blending the CM-PP effectively. The BA worked as a double bond function monomer can promote the formation of micro-crosslinking structure and prevent the degradation of PP molecular chain, which can reinforce the melt strength of PP. It is ascribed to the balance of the strength and strain during the bubble growth.<sup>27</sup> The increase of melt strength can help to retain the gas and avoid the foam collapse. However, when the weight ratio of BA was more than 10 wt %, the cell size and number of foamed PP decreased because the bubbles were difficult to expand with a high melt strength. Therefore, the higher density of crosslinking is not always beneficial due to that the excessive crosslinking would lead to higher stiffness and poorer breaking strain, which will limit the

expansion of the bubbles.<sup>28</sup> The best overall foamability of the CM-PP modified PP with 10 wt % BA might be attributed to the good balance of the strength and strain with moderate enhancement of viscoelasticity.<sup>29</sup>

The cell density is derived from the SEM micrographs. The obtained cell densities of the foamed PP are shown in Figure 6. It can be observed that the cell density of foamed PP increases firstly, the cell density is as high as  $1.33 \times 10^6/\text{cm}^3$  when the PP modified by CM-PP with 10 wt % BA content. It is owing to that the higher degree of crosslinking of PP matrix can prevent the coalescence of cells by strain-hardening of the PP matrix, and lead to more stable cellular structures. When the PP suffers from the plastic deformation during the foaming process, the network formed by crosslinking will limit the movement of PP molecular chain that can improve the melt strength of PP matrix.<sup>29</sup> However, when the BA contents are more than 10 wt %, the cell density of foamed PP decreases due to that the excessive viscoelasticity of PP matrix prevents the formation and expansion of foamed PP bubbles. It indicates

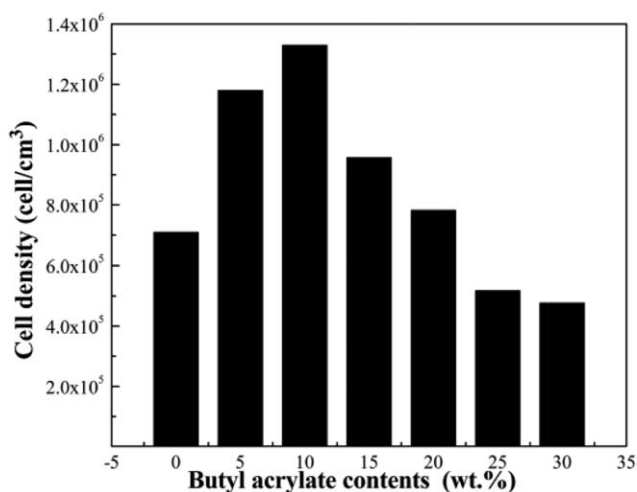


**Figure 6.** Cell density of foamed PP from SEM micrographs with different BA contents.

that the improved cellular structure is directly related to the melt strength of PP matrix. These results are consistent with the result of SEM images.

### Thermal Conductivity

Figure 7 shows the thermal conductivities of PP foam modified by CM-PP with different BA contents. It can be observed that the thermal conductivities of foamed PP decrease from 0.063 W/(m K) to 0.044 W/(m K) as the content of BA increases from 0 to 10%, and then increases to 0.084 W/(m K) with more content BA up to 30%. The lowest thermal conductivity of foamed PP as 0.044 W/(m K) is obtained when the CM-PP was modified with 10 wt % BA content. The thermal conductivities of obtained foamed PP [0.044–0.084 W/(m K)] are much lower than that of unfoamed PP [0.22 W/(m K)], which is attributed to the heat transfer mechanism as follows. First, the solid heat conduction dependent on the lattice vibration is closely related to the density of the solid PP foams. Second, the convective heat transfer relies on the collisions between the pore walls and gas. Third, the radiative heat conduction is an inherent characteristic of the sample, which is rarely affected by the external condition and inherent structure. Herein, the solid heat conduction has been prevented by a decrease of the density as shown in Figure 4, and the convective heat transfer has been cut off by the uniform insular cells because the cross-ventilation has been limited in the insular cellular structures. Furthermore, the gas with extremely low thermal conductivity [ $\sim 0.026$  W/(m K)] in the insular cells will reduce the thermal conductivity of foamed PP effectively.<sup>16</sup> However, when the BA content is more than 10 wt %, the expansion of cells is limited by the improvements of the melt strength, which leads to a continuous solid phase with fewer cells in the PP matrix and an increase of the density with fewer open, connected cells. The continuous solid phase of PP foams increases the solid heat conduction while the open, connected cells provide the convenience for the convective heat transfer, which contribute to increasing the thermal conductivity of foamed PP with BA contents more than 10 wt %. These are in good agreement with the above results of the SEM images and density.

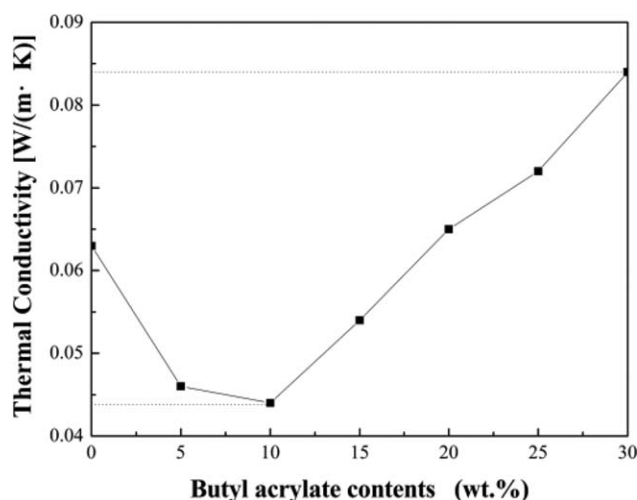


Figure 7. The relationship of thermal conductivities and BA contents.

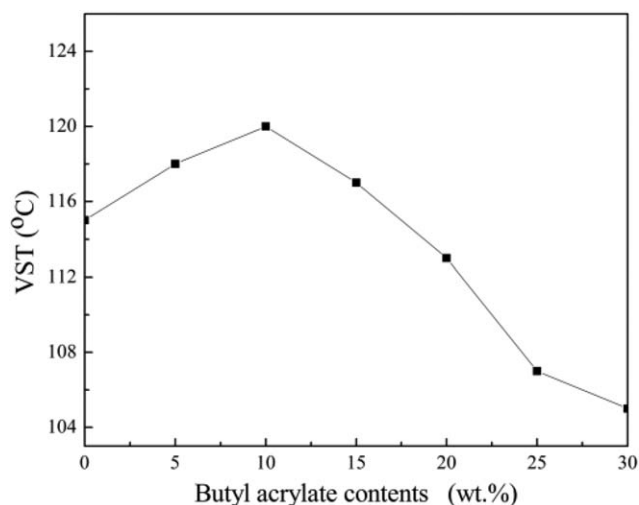


Figure 8. Effects of different BA contents on the VST of foamed PP.

### Vicat Softening Temperature

It is observed that the Vicat softening temperature of the foamed PP increases firstly with an increase of BA contents up to 10 wt %, and the max Vicat softening temperature is obtained as 120 °C, and then decreases with more BA contents as shown in Figure 8. It is mainly due to the uniform insular cellular structure of foamed PP with low density and high cell density, which can cut off the solid and convective heat conductivity effectively.<sup>30</sup> However, when the BA content is more than 10 wt %, the excessive viscoelasticity of PP matrix prevents the formation and the expansion of the foamed bubbles, and the cell density of foamed PP decreases during the expansion process.<sup>6</sup> The increase of density and the decrease of cell density of foamed PP are both not helpful to the thermal insulation.<sup>30</sup>

### CONCLUSIONS

We have presented a new cost-effective technique for the production of foamed PP with excellent thermal insulation by blending CM-PP modified with different contents of butyl acrylate. The results showed that the foamed PP modified with BA had improved the melt strength of PP matrix effectively.

The foamed PP with an optimum performance was obtained by blending CM-PP modified with 10 wt % BA. The SEM images showed that the foamed PP has uniform closed cells with thin solid cell walls, and the density and thermal conductivity of foamed PP were as low as 0.23 g/cm<sup>3</sup> and 0.044 W/(m K), respectively. The cell density and Vicat temperature were as high as  $1.33 \times 10^6$ /cm<sup>3</sup> and 120 °C, respectively. This technology is expected to be applied to the field of high-performance thermal insulator and package.

### ACKNOWLEDGMENTS

This work was financially supported by the Anhui Provincial Department of Education Grant (No. KJ2014A014) and Key Laboratory of Renewable Energy, Chinese Academy of Sciences (No. y407k31001). The authors acknowledge the support from “Anhui Zhongding Sealing Part Co., LTD (Ningguo),” “Institute of High-Performance Rubber Materials & Products (Hefei),” and

“Collaborative Innovation Center for Petrochemical New Materials (Anqing).”

#### APPENDIX

The TCi Thermal conductivity analyzer is a state of the art Thermal property characterization instrument based on the modified transient plane source technique.

The surface' temperature of the inductive probe of the TCi Thermal conductivity analyzer changes with an established current supplied. The temperature rises will lead to an increase of the temperature of the interface between the sensor and sample, and the voltage also changes accordingly, which will be detected by the induction coil on the surface of the sensor. Respond to the temperature rise, the voltage changed. It can identify the thermal property of the sample with the voltage rise rate. According to the data model, the thermal conductivity of the sample will be measured directly.

#### REFERENCES

1. Ester, L. G.; Rob, V. H.; Paula, M. *Appl. Polym.* **2015**, *33*, 132.
2. Yang, J.; Li, P. J. *Reinf. Plast. Compos.* **2014**, *7*, 34.
3. Liu, Z. F.; Li, Y. N. *Eng. Plast. Appl.* **2015**, *3*, 43.
4. Bao, J. B.; Weng, G. S.; Zhao, L.; Liu, Z. F.; Chen, Z. R. *J. Cell. Plast.* **2014**, *50*, 4.
5. Zhai, W. T.; Wang, H. Y.; Yu, J. *Polym. Eng. Sci.* **2008**, *7*, 48.
6. Bai, G.; Guo, C. G.; Li, L. P. *Constr. Build. Mater.* **2014**, *50*, 148.
7. Gen, C. Z.; Ja, K. B. J. *Anal. Appl. Pyrolysis* **2012**, *12*, 96.
8. Parent, J. S.; Bodsworth, A. *Polymer* **2009**, *1*, 50.
9. Passaglia, E.; Coiai, S. *Prog. Polym. Sci.* **2009**, *9*, 34.
10. Li, Y.; Yao, Z.; Chen, Z. H.; Qiu, S. L.; Zeng, C. C.; Gao, K. *Polymer* **2015**, *70*, 207.
11. Liu, H.; Chuai, C. Z. *J. Appl. Polym. Sci.* **2011**, *2*, 122.
12. Feng, J. M.; Wang, W. K. *Polym. Plast. Technol. Eng.* **2011**, *10*, 50.
13. Sun, Y.; Ueda, Y. J. *Supercrit. Fluids* **2015**, *2*, 103.
14. Liu, T.; Zhou, S. Y.; Lei, Y. J. *Ind. Eng. Chem. Res.* **2014**, *51*, 53.
15. Shen, C. J.; Lu, G.; Yu, T. X. *Int. J. Impact Eng.* **2014**, *74*, 92.
16. Guo, P.; Xu, Y. H.; Lu, M. F.; Zhang, S. J. *Ind. Chem. Res.* **2015**, *1*, 54.
17. Zhang, Y.; Tiwary, P.; Parent, J. S.; Kontopoulou, M.; Park, C. B. *Polymer* **2013**, *54*, 4814.
18. Su, L. F.; Miao, L.; Tanemura, S. *Sci. Technol. Adv. Mater.* **2012**, *13*, 035003.
19. Su, L. F.; Zhang, W.; Xia, R. *Adv. Mater. Res.* **2015**, *1090*, 50.
20. Wang, H. Y.; Hu, X. T. *Prog. Chem.* **2007**, *6*, 19.
21. Spital, P.; Macosko, C. W. *Polym. Eng. Sci.* **2004**, *11*, 44.
22. Bao, J. B.; Junior, A. N.; Weng, G. S.; Wang, J. J. *Supercrit. Fluids* **2016**, *111*, 63.
23. Babu, R. R.; Singha, N. K.; Naskar, K. *Exp. Polym. Lett.* **2010**, *4*, 4.
24. Lee, S. J.; Zhu, L.; Maia, J. *Polymer* **2015**, *70*, 173.
25. Li, Y.; Yao, Z.; Chen, Z.; Cao, K.; Qiu, S.; Zhu, F. *Chem. Eng. Sci.* **2011**, *16*, 66.
26. Auhl, D.; Stange, J.; Münstedt, H.; Krause, B. *Macromolecules* **2012**, *11*, 51.
27. Kumar, P.; Topin, F. *Int. J. Heat Mass Transfer* **2016**, *92*, 539.